ISSN 2348-9928
Doi:10.46532/ijaict-202108029 Published on 05 (10) 2021

Big Data Techniques for Clinical Image Analysis

[1]Hang Ying and [2]Qin Yu
Department of Biomedical Engineering, Zhejiang Chinese Medical University, Hangzhou, China.
[1]hangying395@gmail.com

ArticleInfo
International Journal of Advanced Information and Communication Technology
(https://www.ijaict.com/journals/ijaict/ijaict_home.html)
https://doi.org/10.46532/ijaict-202108029
Received 12 April 2021; Revised form 26 June 2021; Accepted 28 August 2021; Available online 05 October 2021.

Abstract - The process of extracting clinical images, for instance, heart images from cameras is full of noises and complexities. As such, the general expenditure for processing these images like resources and time is significantly high, mostly for complex and large amounts of data. In that case, this research contribution utilizes the machine vision-centred method to effectively address these issues. The method significantly incorporates four essential stages with various forms of algorithms to handle the clinical heart images. In the first stage, the smoothing algorithm is utilized to minimize some form of noise. In the second stage, the filtering algorithms are applied for the analysis of images to effectively identify the targeted region. In the third stage, more developed algorithm is utilized to evaluate the image characteristics in the targeted region, identifying the basic image outline. Lastly, the reduction algorithm is meant to transform the original image into significantly precise and smooth pictures. The experimental findings indicate that the machine vision-centred clinical image analysis algorithm might significantly extract fundamental data and attain the most reliable results, contrasting with the most ancient image analysis techniques.

Keywords - Machine Vision; Heart Image; Clinical Image Processing; Digitalized Image.

1. Introduction

In the field of science and technology, machine vision is considered as a fundamental product that aids in the analysis of images. As an entire discipline, the computing vision framework is considered as an artificial framework theory in science. It is retrieved from image data which might be retrieved using different ways such as camera plurality, video sequences and multiple-dimensional visions which are the methods to attain the computing visioning for image models and theories. The ancient machine vision framework applications incorporate various aspects: (1) control procedure (for instance, the automated vehicles or industrial robots; (2) event detection (e.g. people counting or video surveillance; (3) industrial information (e.g. index data in image sequences; (4) ecosystem and modeling object (e.g. company inspection, topographical modelling and clinical image evaluation); (5) interactions (such as computer-human interaction output-input devices). Significant application of the machine-vision in images, e.g. the production of the 3D computing graphics model information is normally produced from the image information framework via the 3D aspect. The computing vision is centred on even detection, scene construction, video tracking, learning, motion evaluation, target recognition, image retrieval and indexing. Machine vision is a relatively diversified sector in computer visioning. This technology is significantly connected to image processing, machine visioning and image analysis. These connected fields are incorporated in the wide-range applications and technologies using a single basic form of technology [1]. The machine-vision technology typically concentrates on a single or multiple image. For instance, the way 3D projects are structured based on scene data or data from the processed images.

This methodology normally depends on the aspect that the illustrated case in the images surpasses the level of image complexity. In this case, machine visioning is considered as one of the most applicable segments in clinical image processing. The features of the application segments are the data extracted from the patient's clinical diagnostic imaging datasets. In general, information might be retrieved from the microscopic images and considered as x-ray images, ultrasonic mages or contrast images which also includes tomographic images. Information might be retrieved from the images. For instance, tumor detection and arteriosclerosis including other riskier transformations. Information can also be retrieved from the flow of blood, sizes of organs and other essential measurements in the body [2]. The significant data is applicable in the development of the structures of clinical quality. In that regard, the clinical image processing aspect has fundamental and practical relevance in saving the lives of patients. The basic techniques of machine-vision in clinical image processing are categorized as follows: principal component evaluation; linear filtering; independent component evaluation; encrypted Markov framework; partial differentiated equation; neural network; self-organization chart and the wavelet.

Based on the advancements of computing applications, novel approaches are constantly emerging and the level set approach is considerably utilized in machine vision. This approach mainly includes de-noising, image increase, image repair and the assessment of outstanding advantages. The image curve transformation approach is known for accepting and assessing the image data gradient for active contour framework. The framework is capable of extracting more complex shapes of targeted images and the vital outline of the contours. The degree of sensitivity is considerably minimized [3]. To effectively mitigate the challenges of the approach, the function will rely on the

Corresponding author at: Hang Ying, Zhejiang Chinese Medical University, Hangzhou, China.

sighed distance element which is a novel variation formula utilized to eliminate the process of re-initialization. This might possibly enhance the velocity of the curve evolution.

Lastly, it minimizes the over complexity of approach's function. Clinical heart images, utilizing the approaches of machine vision have been evaluated in this research through the application of novel methods. The method is basically grouped into the steps that follow: edge-adapted smoothing algorithms which are applicable in the heart imaging process to eliminate noises; the mean filter algorithm that is applicable in the process of analyzing images and utilized when identifying targeted image regions; enhanced algorithm which is applicable to retrieve images from the targeted region characterization and to note the basic elements of images and image restoration algorithms which are utilized in the creation of images based on the application of the 3D framework [4].

2. Background Analysis of Deep Learning (DL)

2.1 Machine Learning (ML)

The basic application of ML-centred image segmentation technique is to categorize the regions of interest such as healthy parts or the diseased parts. The procedures and steps included for the creation of the application starts from the pre-processing stages that might include the usage of the filters meant to eliminate noises. This might also be due to contrast development of images. Based on the stage of pre-processing, images are segmented following the application of the segmentation approach such as clustered-centred method, thresholding method and the edge-centred segmentation process. After the process of segmentation, the characteristics are retrieved in reference to texture, colour data, size and contrast from the region of interest. The dominant characteristics are identified based on the application of characteristics selection approaches such as the Principal Component Analysis (PCA) or the statistical evaluation. Subsequent to that, the chosen characteristic is utilized as the input to the machine learning categorized of NN and SVM. ML categorizer makes use of the input characteristic vector alongside the targeted label to effectively identify the optimal boundary which separates every category. Whenever ML categorizer has been trained properly, it might be utilized to categorize novel unconfirmed information to evaluate its category. The normal challenges incorporate the evaluation of the effective pre-processing necessities in reference to the raw image features, identification of effective characteristics and characteristics vector lengths including the forms of classifiers.

2.2 DL-Centred Categorizer (DLC)

DLC is capable of processing raw images in a more direct manner. This shows that there has to be no pre-processing or feature extraction processes. Nonetheless, a lot of DL methods necessitate image restructuring as a result of the limit included in the input value. Whereas a number of approaches do not necessitate intensified contrast and normalization developed that might be eliminated when information augmentation approaches are used that might be applied in the process of image training. As a result, DLC is known to have higher categorization efficiency since it might potentially eliminate all the mistakes connected with the incorrect characteristics vector or the imprecise image segmentation. The contrast of DLC and ML methods is considered in Fig 1 below. DLC-centred methods have also transformed the perspective of the analysis from ancient image segmentation methods for characteristic engineering to a more networked structural design that makes it possible to obtain optimum results. DLC networks normally have a lot of hidden layers that significantly implies more mathematical calculations being done in contrast to ML-centred methods and therefore the frameworks are considered computationally intensified [5].

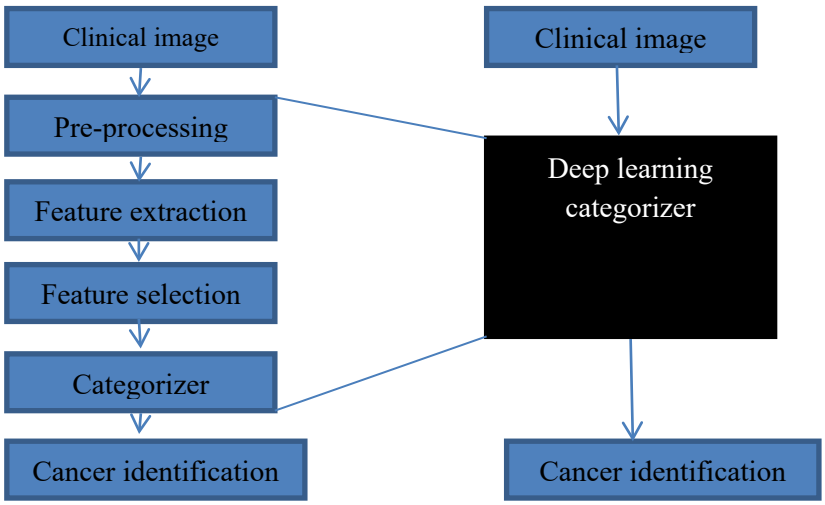

Fig 1: Transformation in the categorizer method based on the application of ML algorithms and DL

As indicated from Fig 1, the ML categorizer considers the element vector as the output and input which is object category and the DL categorizer considered in the image output is object category. It might be considered that the DL categorizer is the development of the common Artificial Neural Network (ANN) since it included more layers compared to ANN. Moreover, it is known as a form of representational ML since every layer changes the input information from the initial layer into a novel representation as a significantly higher level of abstraction [6]. This permits the framework to master both international and localized connections of the complete data in a more hierarchical framework. The transition of information in the kind of representation in every layer of DL framework is due to non-linear elements. Typically, element extraction of images from the initial representation layer for a certain image might identify the absence or presence of edge in certain location and alignments in images. The second layer is capable of detecting the patterns through the process of identifying the position of edges and eliminates minor variations of these locations whereas the third layer connects these patterns into significant linkages that connect to the object fragments whereas allowing the succeeding layers to effectively identify the objects based on these linkages. The hierarchical element representation from ML and data evaluation has amounted to the unprecedented effectiveness of DL in significant AI applications.

3. The Architecture of DL – Convolutional Neural Networks (CNNs)

In lot of DL architectures, CNNs are widely applied due to the fact that they are the same as the conventional NNs. As projected to the normal form of NN, indicated in Fig 2a, CNNs considers images as inputs with 3D dimensional connection of various neurons which linkup with minor regions of the common preceding layer other than the complete layer that is indicated in Fig 2b below. CNNs include the layers such as non-linear layer of activation, convolutional layer, completely connected layer and the pooling layer. In the convolutional layer, the operators of convolution in the input image pixels are included with the filters meant to obtain the volumes of the element map with characteristic retrieved by the wide-range filters. The Rectified Linear Unit (ReLU) layers are collectively known as the non-linear layers of activation which apply the element function of f (x)=max (0, x) to the input figures to enhance the velocity of the training and non-linearity [7].

The pooling layers significantly samples the values of the input to minimize the spatial dimension of images to enhance the cost of computation and to limit overfitting. These are considered a translation invariant in the process of computation in relation to the closer pixels. The completely linked layers are known as the final layers of CNNs and are considered the same as the encrypted layers of the ancient NN in the aspect that the neurons in the layers are connected to those neurons available in the preceding layers. As discussed earlier, CNNs are normally utilized for the categorization of issues. To utilize CNN for the process of semantic segmentation, input images are divided into minor segments of the same size. CNNs classify the pixel centre in various patches which are later glided to categorize the pixel center. Nonetheless, this method is considered inefficient just like the overlapping element of the sliding patch which are not re-utilized hence amounting to the absence of spatial data of images as characteristics are known to shift from the last completely connected network layer [8]. To mitigate this issue, the application of completely convolutional network has been projected whereby the last completely linked layer of CNNs has been transformed to effectively transpose the convolution layer as indicated in Fig 2c. The layer applies the up-samples on the minimal-resolution feature map which effectively covers the initial spatial dimension whereas effectively performing a semantic subdivision.

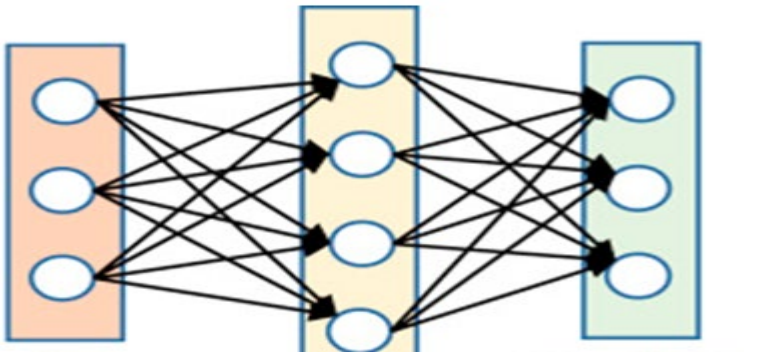

(a)

Corresponding author at: Hang Ying, Zhejiang Chinese Medical University, Hangzhou, China.

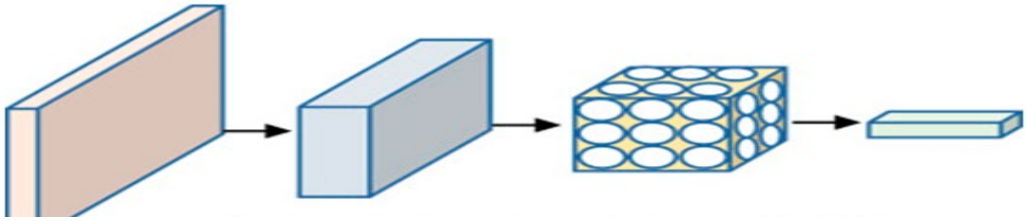

(b)

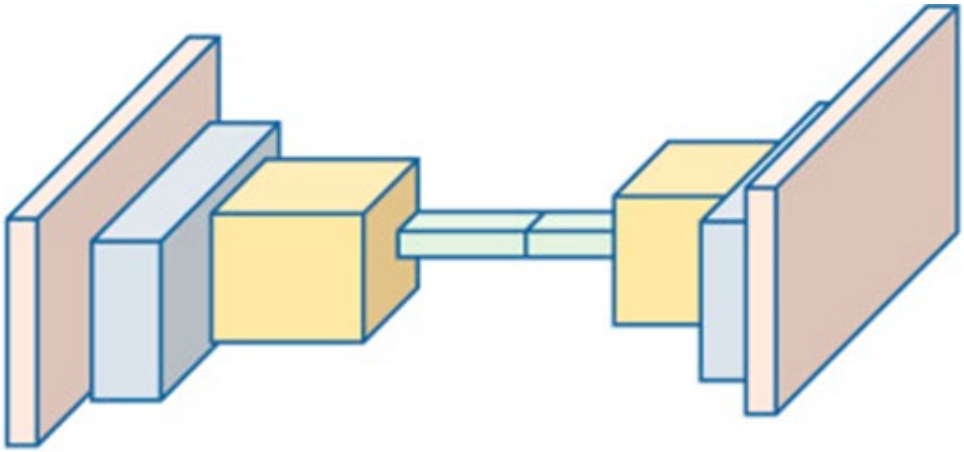

(c)

Fig 2: (a) NNs layers (one encrypted with four neurons and another with the output layers with three neurons and three inputs; (b) CNNs and; (c) Completely Convolutional Networks (FCNs)

Normally, the DL neural network is effectively trained based on the application of the back-propagation algorithms that links up with the optimized algorithm just like the gradient descent. The procedure includes the gradient determination of the absence element that is applied by the optimization algorithm to effectively update the weight of the network so as to effectively minimize the absence function figure. Researchers, over the past few years have recommended utilizing the multiple-level DL convolution network for pancreas segmentation that is considered to have considerable anatomical variability. Pancreas segmentation is fundamental for the purpose of quantifying the volume of organs, especially for diabetic patients [9]. Approximately 82 comparison-enhanced abdominal CT volumes alongside the ground truth have been utilized in the research. Moreover, the randomized non-rigid deformation has been applied in the process of retrieving more data cases. The measure of deformation has been chosen to make sure that the warped images require differentiation just like the actual datasets. In the projected bottom-up method, image patches were initially labelled. As for the image patches label, the sagittal, coronal and axial view of these patches have been applied to effectively obtain the locational probability response maps. This has been preceded by the part labelling through the generation of the super-pixel parts with significant level of sensitivity, but minimal precision at various special dimension in the zoomed method. CNNs were utilized to allocate the required probability to every super-pixel as a pancreas tissue. Lastly, the complete organ was identified from the abdominal CTs scans that apply both the CTs

Corresponding author at: Hang Ying, Zhejiang Chinese Medical University, Hangzhou, China.

intensity figures and the probability response maps retrieved from the super pixel parts.

Medical researchers have also recommended the application of the completely convolutional networks whereby the various layers of CNNs were either pooling or convolutional for the purpose of segmenting the liver from 3D CT scan, vessels and whole heart from MR images. This method was essential to eliminate the size limit of input of images to networks that were available as a result of the completely interlinked layers. The inclusion and transformation of the completely interlinked layers with the convolutional layer shows that the input images might possess the arbitrary categorization output and sizes might spatially be arranged from the complete input images. This might significantly eliminate the requirement of the redundant computation level amounting from the overlapped region in the ancient patch-centred method. 3D DL supervision approach typically extracts the characteristic map from the encrypted layer before upscaling them by linking them to the deconvolutional layer which also incorporates the SoftMax function to effectively obtain high density projections. The function of SoftMax is capable of performing an exponential normalization of the input vector including the actual figures before transforming them to the probability distribution like that of the output figures which are in the (0,1) intervals with the summation of output figures amounting to 1. The categorization error of the branched output contrasts with the actual ground truth which is utilized to transform the network parameters in the mainstream network during the process of training.

The researchers have also recommended the patch-based multiple atlas approach which has been linked with the voting approach with CNNs for properly segmenting regions in the MRI deep brain and the US images. This method might significantly segment structures even when there are partially corrupted or visible as artifacts. CNNs are trained to categorize the background and foreground parts in the patches that are retrieved from the voxels and connect every input to their relative feature representation retrieved from the last completely linked layers. The protocol is therefore repeated for completely training information and datasets are produced to contain 3D, 2.5D and 2D patch for the foreground parts and the element extraction [10]. The 2.5D includes the significantly higher spatial data of the closer neighboring pixel and it is normally obtained based on the application of the 3D orthogonal patch (XZ, YZ and XY plane) which incorporates the resultant kernel in 2D.

Moreover, votes are gathered with the vector displacement that links the positional anatomy and the voxels centroid. This is considered as the same voxels whereby the patches have been gathered. In the process of testing, CNNs which produce the labels for corresponding characteristic maps and the unknown voxel for the different patches are labelled as foreground in the process of extraction. Every feature map is contrasted with the feature map in the available database to retrieve the k-next neighbours in reference to the Euclidean distances. These votes of the corresponding and closer subdivided patches are utilized to conduct segmentation and the procedure is done again for the various foreground patches. This approach is considered superior to the voxels semantic subdivision of CNNs in the various parameter settings being evaluated. This also includes the parameters that necessitate fewer training information that produced effective segmentation contour and removed the necessities for conducting post processing [171].

The researchers have also proposed the voxel-centred DL framework centred on the residual network considered as the VoxResNet. Normally, DL framework creates the feature representation framework in a more successive manner with level transformation at low-to-middle-high. A significant portion of layer which incorporated the networks implies more data that needs to be learned therefore enhancing the capacity of discrimination of networks. However, this might not always happen during the performance time that begins to degrade at a significantly deeper network layer. This is considered as the degradation issue and ResNets is considered to mitigate this issue as residual education aids the process of network optimization to become significantly easier and is accomplished through the application of skipped connections. As such, data might be spread via the complete network both in backward and forward pass.

To effectively address the volumetric information for the segmentation of the brain from three-dimensional magnetic resonance, VoxResNet was recommended to surpass 3D and 2D ResNet. The projected network includes the stacked residual module. As for the VoxRes framework, the changed element and input features are incorporated inclusively with the skipped connections. To effectively address the variation size of the 3D anatomy brain system, 4 auxiliary categorizers C1 to C4 are applied for the purpose of fusing multiple-level contextual data. In the 1st layer of a network, data from many modalities which gave complementary data on the same brain structure was linked to the data weights in the phase of training. This amounted to the enhanced efficiency contrasted to the findings obtained via the single form of modality.

The application of the Deep Weak Supervision (DWS) has also been recommended under the aspect of the Multi-Instance Learning (MIL) methodology. In this methodology, during the process of training the categorizer cases are classified inclusively and considered as bags. Every bag is therefore allocated a negative and positive label in the process of training. However, the cases are not allocated any form of label. MIL approaches necessitate that the categorizer framework has to be capable of predicting not just the level of instances but also has to undertake or launch the bag-level categorizer. Based on the perspective of the histopathology image, every non-cancer and cancer image might be known as a bag whereas every pixel in the images is known as a pixel [12].

Normally, a categorizer predicts the level pixel and label whereby the image-level predictions are evaluated based on the application of the SoftMax element or the normalized exponential element. DWS method utilizes the

Corresponding author at: Hang Ying, Zhejiang Chinese Medical University, Hangzhou, China.

multi-sided output retrieved from CNNs normally after the layer of convolution which is usually the manner in which data was retrieved for the purpose of fusion. The purpose of DWS is to make sure that minimum prediction mistakes between the ground truth and every side truth amounts to more enhanced performance. The two considerable methods were linked to create a novel framework known as DWL MIL. Moreover, another issue that happens in most cases is the jagged boundary of tissue which amounts from the handled pixel of cases. The application of the super pixel as a case was recommended to mitigate this problem and diminishes the case numbers hence minimizing the complexity of computation.

4. The Machine-Vision Clinical Image Processing

The cardiac clinical image retrieved by the specialized machines included rich, defined texture and the data complexity which are represented as a heart. However, when this is retrieved from the specialized tool, the image incorporates artifacts and noises. The artifacts and noises are not just some factors influencing the texture findings, but also affects the implication of the kind of judgement on the regions attacked by the heart illness. Therefore, it is fundamental to evaluate the initial heart image. The machine-vision clinical image processing method incorporates four fundamental steps that are defined as follows:

4.1 Step 1: Smoothening

The ancient image smoothening algorithm includes the Gaussian smoothening approach which includes the Gabor and Mean Smoothing. As such, the Gaussian smoothing aspect makes use of the Gaussian element and function.

$$f(x) = ae^{\frac{(x-b)^2}{2x^2}} \quad (1)$$

The approach makes use of the Gaussian element and function to constitute the minimal pass filter in the domain of the image frequency. The filters have smoothing performance of multi-applications for this aim. The mean smoothening approach makes use of the non-linear approach to access the mean value off from the N pixel. The Gabor smoothening approach makes use of the Gabor element to effectively localize the time frequency in a more precise manner which considers adopting the Gabor window critically for this aim [13]. The non-linear smoothening algorithms are recommended in this paper to effectively process and structure the clinical images. The algorithms are related to the localized which continuously measure discontinuity texture to effectively obtain the mean quantization of smoothing images.

$$Exy = E_{H_{xy}} + E_{V_{xy}} + E_{D_{xy}} + E_{C_{xy}} \quad (2)$$

Whereby

$$E_{H_{xy}} = I_{x+I,y} - I_{x-I,y} \ldots . E_{YX} = I_{x,y+1} - I_{x,y-1}$$

$$E_{D_{xy}} = I_{x+I,y} - I_{x-I,y} \ldots . E_{YX} = I_{x,y+1} - I_{x,y-1}$$

The cardiac clinical images are based on the pixel gray level with a number of differential forms of deviation. A number of gray figures of images are typically influenced by the image noises. However, the data of every pixel in image fields might minimize the implication. The projected smoothening algorithm evaluates the gray variance and mean mathematically based on the discontinuity quantitative texture. In that case, it is considerably easier to obtain the below expression:

$$\sigma_{xy}^{-2}(R) = \frac{\sigma_{xy}^{2}(R) - \sigma_{min}^{2}(R)}{\sigma_{max}^{2}(R) - \sigma_{min}^{2}(R)} \quad (3)$$

$\sigma_{xy}^{-2}(R)$ form the discontinuity of (x, y). Considered $\sigma_{xy}^{-2}(R)$ as the threshold figure, the smoothening algorithm formulae can be illustrated as

$$\emptyset(\sigma_{xy}^{-2}(R), \theta_\sigma = \begin{bmatrix} 0 & \sigma_{xy}^{-2}(R) < 0_\sigma \\ \sigma_{xy}^{-2}(R) & \sigma_{xy}^{-2}(R) \geq 0_\sigma \end{bmatrix} \quad (4)$$

4.2 Step 2: Mean Filtration

The actual mean filtration algorithms are centred on the projected methods from Hart and Duda. These methods make use of the error square dynamics clustering approach to effectively process the images. As for the cardiac images mostly evaluated in this research, it considers the function which is adopted for the filtration of the general mean.

$$j_c = \sum_{j-l}^{c} \sum_{k-l}^{nj} \left\| X_k - m_j \right\|^2 \quad (5)$$

Whereby e, $m_j = \frac{1}{n} \sum_{k-l}^{nj} X_k \quad j = 1,2, \ldots . c$

For image smoothing, the wide-range pixels are in their initialized clustered centre, denoted by c. The choice of c is accorded to the data content allocated for the images. Once the various experiments have been done, the fixed figure of 16 is selected. This shows that every cluster includes an approximation of 16 pixels. Considering the four-point figure as the general mean, mj is considered as the lean figure in the number j category. Using the approach, it is considerably comparing the grayscale pixel value in the images. In that case, the purpose of advancing the contrasted targeted region and the remaining image parts is considerably accomplished. This is the basis in the step of image processing which is known as image enhancement.

4.3 Step 3: Image enhancement

The cardiac clinical image texture is based on the abundance of data. The enhancement of images not just connects to the heart detail development, but also reflects on the complete texture data result in a certain degree. This contribution plays fundamental role and the relevance of processing these image textures are related to the texture value of the image data. In that case, the image contrast, C x y, is identified by the texture data f u x y.

$$C(x,y) = \frac{|u_f(x,y) - \bar{u}(x,y)|}{|u_f(x,y) + \bar{u}(x,y)|} \quad (6)$$

Corresponding author at: Hang Ying, Zhejiang Chinese Medical University, Hangzhou, China.

Whereby $u_f(x,y)$ is considered as

$$u_f(x,y) = \sum_{i-x+\frac{k-1}{2}}^{x+\frac{k-1}{2}} \sum_{j-y+\frac{k-1}{2}}^{y+\frac{k-1}{2}} [u(i,j) * \sigma(x,y)] \quad (7)$$

Based on the application of the image development algorithms, the comparison development of the heart image reflects not just the international pixel data, but also evaluates the localized details of the image data. The detailed partial data is reflected based on the weighted function which is considered to be more enhanced by the pixel of images and their intensity. The element and function are a manner of user-illustrated localized enhancement of various image forms. The exponential element and function are utilized for this aim.

$$\sigma(x,y) = x \sum_{k=0}^{1} \frac{p}{\sum_{k=0}^{1} pi} ln \frac{pi}{\sum_{k=0}^{1} pi} + y \sum_{k=0}^{1} \frac{p}{\sum_{k=0}^{1} pi} ln \frac{pi}{\sum_{k=0}^{1} pi} \quad (8)$$

From the above equation, p is considered the statistical number and probability in the complete image grayscale. The weighting approach is utilized to enhance the targeted area and the comparison of other parts which provides the most essential data for the last step in the reduction of the image.

4.4 Step 4: Image Restoration

Image restoration is the final step. The algorithm for this step is centred on the aspect of machine vision not just the structural features, but also the texture data that has properly been grasped. Mostly, it is considered effective and efficient for colour transformation contour and visible parts with effective robustness. As for the coloured heart clinical images centred on the texture data structure pixels, the weight setting is done to enhance the level of accuracy in images which can considerably be enhanced to form colour balance [14]. Image similarity in the process of restoration is illustrated as shown below:

$$d(\emptyset_x, \emptyset_y = \sum_{i,jc\emptyset nuf(x,y)}^{n} W(i,j) * L(x,y) \quad (9)$$

From the above equation φ is considered the restored pixel block. W i j (,) is considered the overall weight. L x y (,) is termed the overall square sum and variation from the degree of colour. In that case, the restoration of images and formula might be done with reference to the below expression.

$$L(x,y) = [r(x,y) - R(x-l, y-1)]^2 + [G(x,y)] - [G(x-1, y-1)]^2 + [B(x,y) - B(x-1, y-1]^2 \quad (10)$$

In the expression R,G,B signifies the element value of blue, green and red.

5. Experiments and Discussion

In this analysis, the experiments are centred on cardiac clinical images. The projected approach has been borrowed on image processing. Matlab 2008(a) is applied for this process. The PC ecosystem is the HP Compaq Core 2 with the Central Processing Unit of 6600 at 2.39GHZ, 2.40GHZ which also includes 3GB RAM. The kind of images utilized in the experiment originates from 1024 by 768 colours of pixels of the cardiac clinical image. In this experiment, the initial image is represented in Fig 3 and presents the kind of image that is obtained based on the application of the special tool, but based on the availability of noises. The fundamentally rich textures of images have been considerably obvious and not entirely prominent. In that case, it is not present in clinical professional aspect of image data that has been represented by accurate diagnosis such as myocardial necrosis and coronary heart illness. It is fundamental to conduct image process before undertaking any form of diagnosis.

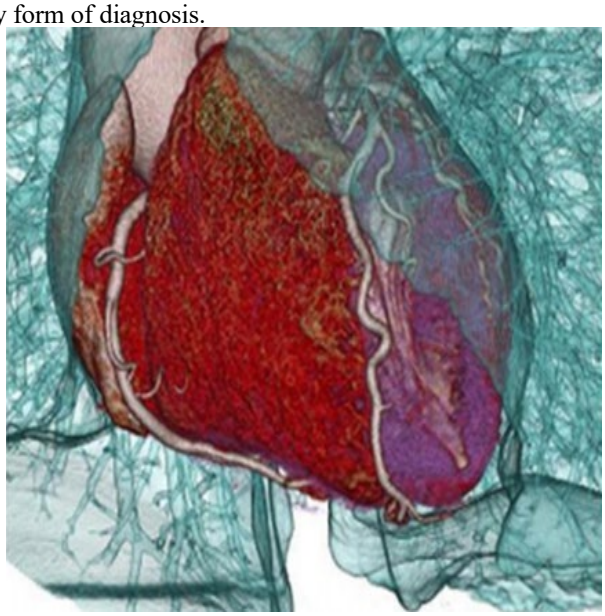

Fig 3: Original heart image

Based on the application of the projected filtering and smoothing algorithm, Fig 4 signifies four critical images based on various dimensions retrieved after filtering and smoothing processes of the projected algorithms for the processing of images. The two images represent the kind of images retrieved after smoothing algorithms. It might be visualized that the images produce negative and positive results after the process of smoothing is complete and has considerably minimized most noises. Moreover, negative and positive (i.e., the images are inverted 180 degree) in the process of smoothing due to the fact that the data of the heart images might be presented as well, mostly the cardiac or vascular subtle texture. In case the single but smooth one is utilized; essential data might be eliminated.

Corresponding author at: Hang Ying, Zhejiang Chinese Medical University, Hangzhou, China.

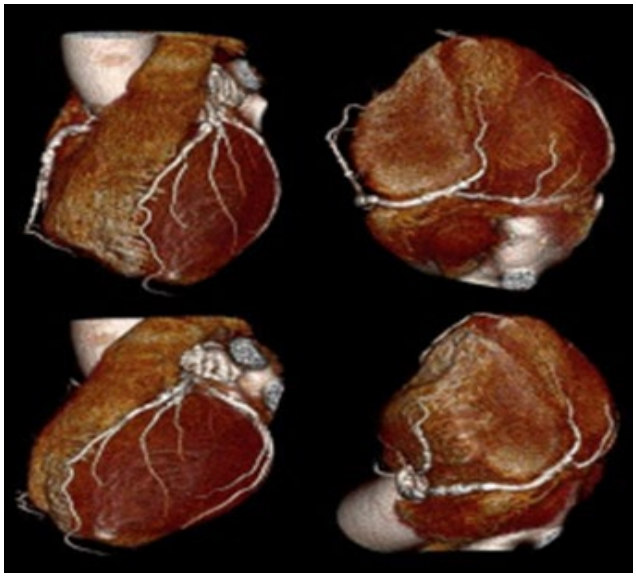

Fig 4: Images after filtratiation and smoothening

The two fundamental images from the bottom in Fig 2 included the coloured images following the process of filtration. Contrasted to the above figure, whereby texture elements the texture parts or arteries have their prominent elements removed. This is probably due to the process of filtration which typically utilizes the filtration algorithm pixel to effectively process images. The squared mistakes of pixel clustered are evaluated mathematically. In that case, the critical focus regions of the image texture features are highlighted. After this, it is fundamental to incorporate the mean absolute distance which will describe the smoothened image filters and pixel difference that typically uses the formula below:

$$Mad(P,M) = \frac{1}{2}\left[\frac{1}{n}\sum_{i-1}^{n} d(pi,M) + \frac{1}{k}\sum_{j-1}^{n} d(mj,P)\right] \quad (11)$$

Whereby

$P = (p_1, p_2, \ldots p_n), M = (m, m_2, \ldots m_n), d(p_1, M) = min\|m_i - p_i\|$

From Fig 4, the connected parts are considered concentrated after the process of filtration based on the details of the distant images. The approach not just amplifies the data area, but typically retrieves more featured values from the process of observation. Fig 3 above indicates the colour effect after the enhancement of images based on the application of the projected enhancement algorithms. It is evident that the image projection and focus region, including the prominent characteristic values (myocardial texture, blood vessels) are considerably weighted.

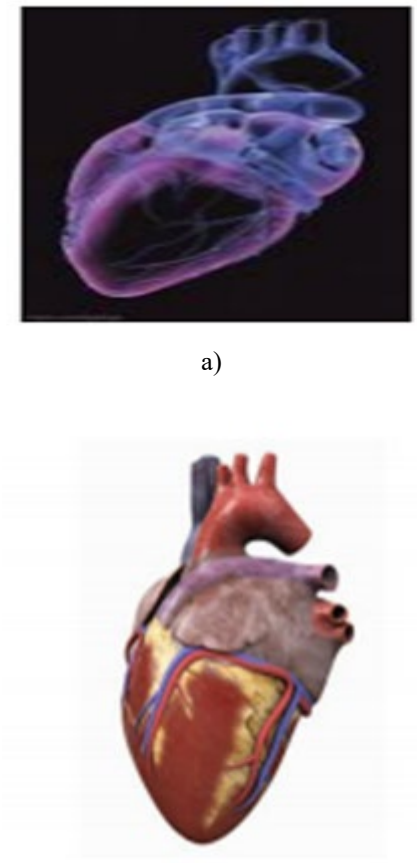

a)

b)

Fig 5: a) Image after enhancement b) Image after restoration

The values are utilized for the purpose of enhancing the images. Other parts, such as the smoothing cardiac weights are incredibly diminished, hence obtained the required display results. It is considered that the method defines the highlighted impact of the heart clinical images: ventricular nerves and ventricular arteries [15]. Fig 5b indicates the retrieved images following the application of machine vision-centred algorithm. This is visualized from the figure, whereby the approach might not just restore the heart image by various regional blocks to signify the initial image, but significantly highlights the walls of the relative vessels of blood in the heart tissue.

The application of coloured RGB in the minimized basic element significantly reflects the real image of the myocardial structure and texture of organizations hence attaining the most effective form of restoring images. Based on the four-step approach of image processing in clinical image processing discussed in this contribution the experiments have considerably outperformed various ancient approaches. The algorithms at the clinical heart image processing measure makes use of the steps evaluated in this paper for machine vision. Image smoothening algorithms, restoration algorithms, enhance and filtering algorithms are incorporated in the four-step method that can considerably mitigate the accessibility of the heart in

Corresponding author at: Hang Ying, Zhejiang Chinese Medical University, Hangzhou, China.

clinical imaging of certain instruments. The experiment findings indicated that it might accomplish the desired image effect.

6. Conclusion and Future Directions

This paper discusses the method for clinical colour image processing (with the samples of the heart retrieved by custom tools). The method includes four fundamental steps. In the first step of processing, the smoothening algorithms are meant to eliminate the artifacts and noises in the images. After that, the image smoothening is illustrated by the filtration algorithm that does the entire process of filtration. The usage of the image distance difference approach is to enhance the effects of the entire filtration process. Subsequent to that, the image enhancement algorithms make use of the weighted developed images for various regions of interest. Lastly, the restoration algorithms are utilized in the process of restoring the colour images for the organ. The experimental findings indicate that the projected step and approach might be applied to accomplish effective image effects. Future directions in the same research are based on different aspects. Firstly, the experimental usage of the sampled images might be based on the contrast algorithm which significantly necessitates more research. Secondly, the image restoration algorithms for clinical image data of the entire organ are based on efficiency. However, the transformations in the heart muscle and gradient necessitates more detailed research in the future. Lastly, interlinked research about the organ is considered insufficient according to this paper. Therefore, the cases of the recommended algorithms and the manner to conduct the research extension and in-depth evaluation should be considered as well.

References

[1]. Z. Zhang and L. He, "Whiteboard scanning and image enhancement", Digital Signal Processing, vol. 17, no. 2, pp. 414-432, 2007. Available: 10.1016/j.dsp.2006.05.006.

[2]. A. Farley and J. Shah, "Primary considerations for image enhancement in high-pressure scanning electron microscopy", Journal of Microscopy, vol. 158, no. 3, pp. 389-401, 1990. Available: 10.1111/j.1365-2818.1990.tb03010.x.

[3]. O. Wells, "Scanning reflection image from a solid specimen in the scanning electron microscope with a condenser-objective lens", Scanning, vol. 10, no. 2, pp. 73-81, 1988. Available: 10.1002/sca.4950100204.

[4]. J. Martin, G. Jenkinson and D. Bulgin, "Quantitative scanning electron microscopy using integrated digital image store for on-line image analysis", Scanning, vol. 7, no. 5, pp. 239-242, 1985. Available: 10.1002/sca.4950070504.

[5]. H. Le Floch, J. Franceschi, T. Gouraud and P. Launay, "Digital image acquisition in scanning electron microscopy", Scanning, vol. 9, no. 1, pp. 26-30, 1987. Available: 10.1002/sca.4950090105.

[6]. R. Edwards, J. Lebiedzik and G. Stone, "Fully automated SEM image analysis", Scanning, vol. 8, no. 5, pp. 221-231, 1986. Available: 10.1002/sca.4950080505.

[7]. K. Jenkins, "Quantitative image mode voltage contrast", Scanning, vol. 9, no. 5, pp. 194-200, 1987. Available: 10.1002/sca.4950090503.

[8]. G. Rosolen and W. King, "An automated image alignment system for the scanning electron microscope", Scanning, vol. 20, no. 7, pp. 495-500, 1998. Available: 10.1002/sca.1998.4950200702.

[9]. A. Sasaki and J. Fukaya, "Microstructure-image enhancement by scanning photoacoustic microscopy", Journal of Applied Physics, vol. 66, no. 1, pp. 455-456, 1989. Available: 10.1063/1.343849.

[10]. T. Kirk, L. De Pietro, D. Pescia and U. Ramsperger, "Electron beam confinement and image contrast enhancement in near field emission scanning electron microscopy", Ultramicroscopy, vol. 109, no. 5, pp. 463-466, 2009. Available: 10.1016/j.ultramic.2008.11.009.

[11]. A. Farley and J. Shah, "Primary considerations for image enhancement in high-pressure scanning electron microscopy", Journal of Microscopy, vol. 158, no. 3, pp. 379-388, 1990. Available: 10.1111/j.1365-2818.1990.tb03009.x

[12]. O. Wells and R. Savoy, "Enhancement of type-2 magnetic contrast in the base image in the SEM by a lock-in technique", Scanning, vol. 2, no. 4, pp. 255-256, 1979. Available: 10.1002/sca.4950020408.

[13]. H. Wickramasinghe and J. Heiserman, "Image enhancement in the scanning acoustic microscope using analogue filters", Electronics Letters, vol. 13, no. 25, p. 776, 1977. Available: 10.1049/el:19770549.

[14]. C. Overbeck, Varadhan and S. Hui, "TU-D-L100J-08: Image Quality Enhancement in MVCT Scanning", Medical Physics, vol. 34, no. 618, pp. 2555-2555, 2007. Available: 10.1118/1.2761372.

[15]. G. Woltmann, A. Wardlaw and D. Rew, "Image analysis enhancement of the laser scanning cytometer", Cytometry, vol. 33, no. 3, pp. 362-365, 1998. Available: 10.1002/(sici)1097-0320(19981101)33:3<362::aid-cyto11>3.0.co;2-r.

Corresponding author at: Hang Ying, Zhejiang Chinese Medical University, Hangzhou, China.